N-terminal pro-B-type natriuretic peptide and subclinical brain damage in the general population

Zonneveld, Hazel I.; Ikram, M. Arfan; Hofman, Albert; Niessen, Wiro J.; Van Der Lugt, Aad; Krestin, Gabriel P.; Franco, Oscar H.; Vernooij, Meike W.

DOI
10.1148/radiol.2016160548

Publication date
2017

Document Version
Final published version

Published in
Radiology

N-Terminal Pro–B-Type Natriuretic Peptide and Subclinical Brain Damage in the General Population[1]

Hazel I. Zonneveld, MD
M. Arfan Ikram, MD, PhD
Albert Hofman, MD, PhD
Wiro J. Niessen, PhD
Aad van der Lugt, MD, PhD
Gabriel P. Krestin, MD, PhD
Oscar H. Franco, MD, PhD
Meike W. Vernooij, MD, PhD

Purpose: To investigate the association between N-terminal pro–B-type natriuretic peptide (NT-proBNP), which is a marker of heart disease, and markers of subclinical brain damage on magnetic resonance (MR) images in community-dwelling middle-aged and elderly subjects without dementia and without a clinical diagnosis of heart disease.

Materials and Methods: This prospective population-based cohort study was approved by a medical ethics committee overseen by the national government, and all participants gave written informed consent. Serum levels of NT-proBNP were measured in 2397 participants without dementia or stroke (mean age, 56.6 years; age range, 45.7–87.3 years) and without clinical diagnosis of heart disease who were drawn from the population-based Rotterdam Study. All participants were examined with a 1.5-T MR imager. Multivariable linear and logistic regression analyses were used to investigate the association between NT-proBNP level and MR imaging markers of subclinical brain damage, including volumetric, focal, and microstructural markers.

Results: A higher NT-proBNP level was associated with smaller total brain volume (mean difference in *z* score per standard deviation increase in NT-proBNP level, −0.021; 95% confidence interval [CI]: −0.034, −0.007; $P = .003$) and was predominantly driven by gray matter volume (mean difference in *z* score per standard deviation increase in NT-proBNP level, −0.037; 95% CI: −0.057, −0.017; $P < .001$). Higher NT-proBNP level was associated with larger white matter lesion volume (mean difference in *z* score per standard deviation increase in NT-proBNP level, 0.090; 95% CI: 0.051, 0.129; $P < .001$), with lower fractional anisotropy (mean difference in *z* score per standard deviation increase in NT-proBNP level, −0.048; 95% CI: −0.088, −0.008; $P = .019$) and higher mean diffusivity (mean difference in *z* score per standard deviation increase in NT-proBNP level, 0.054; 95% CI: 0.018, 0.091; $P = .004$) of normal-appearing white matter.

Conclusion: In community-dwelling persons, higher serum NT-proBNP levels are associated with volumetric and microstructural MR imaging markers of subclinical brain damage.

Online supplemental material is available for this article.

[1] From the Departments of Epidemiology (H.I.Z., M.A.I., A.H., O.H.F., M.W.V.), Radiology and Nuclear Medicine (H.I.Z., M.A.I., W.J.N., A.v.d.L., G.P.K., M.W.V.), Neurology (M.A.I.), and Medical Informatics (W.J.N.), Erasmus MC, University Medical Center Rotterdam, Room Na28-18, PO Box 2040, 3000 CA Rotterdam, the Netherlands; Department of Epidemiology, Harvard T.H. Chan School of Public Health, Boston, Mass (A.H.); and Department of Imaging Physics, Faculty of Applied Sciences, Delft University of Technology, Delft, the Netherlands (W.J.N.). Received March 15, 2016; revision requested May 2; revision received August 3; accepted August 17; final version accepted August 24. **Address correspondence to** M.W.V. (e-mail: *m.vernooij@erasmusmc.nl*).

About 44 million people worldwide are living with dementia, and every year about 15 million people have a stroke (1,2). The social and economic burden of these diseases is increasingly enormously due to the rapidly aging population. A common substrate between dementia and stroke is the presence of subclinical brain damage, which is partly affected by vascular damage (3). Subclinical brain damage can be assessed noninvasively with magnetic resonance (MR) imaging as volumetric (smaller brain volumes), focal (presence of lacunae and microbleeds), and microstructural (poorer organization of the white matter) measures (4).

In the past few decades, research has been conducted to identify the determinants of subclinical brain damage. Recently, interest in the heart-brain link has been increasing (5). Several clinical studies have related coronary heart disease, heart failure, and atrial fibrillation to an increased risk of dementia and stroke (6–9). Interestingly, cardiac function may already be impaired in a preclinical stage.

Cardiac dysfunction can be evaluated by using serum levels of amino-terminal pro–B-type natriuretic peptide (NT-proBNP), which is a biomarker released in response to myocardial wall stress and excreted by the kidneys (10). NT-proBNP yields information on cardiac dysfunction and overload even in the absence of overt heart disease; therefore, it could serve as a marker of subclinical cardiac dysfunction (11). Although few studies have related NT-proBNP with dementia and stroke (12,13), the association between NT-proBNP with the entire spectrum of imaging markers of subclinical brain damage remains to be elucidated.

Linking these two entities would yield more insight into the heart-brain link, which is essential since both cardiac dysfunction and subclinical brain damage are growing problems in the aging population. Thus, in the current study, we aimed to investigate the association between NT-proBNP and imaging markers of subclinical brain damage on MR images in community-dwelling middle-aged or elderly people who did not have dementia or clinical diagnosis of heart disease.

Advances in Knowledge

- In the general population, subclinical cardiac dysfunction, as reflected by higher serum N-terminal pro–B-type natriuretic peptide (NT-proBNP) levels, is associated with global MR imaging markers of subclinical brain damage (difference in standardized total brain volume per standard deviation increase in NT-proBNP level, −0.021; $P = .003$), driven by gray matter volume (difference in standardized gray matter volume per standard deviation increase in NT-proBNP level, −0.037; $P < .001$), and white matter lesion (WML) volume (difference in standardized WML volume per standard deviation increase in NT-proBNP level, 0.090; $P < .001$).
- We showed that serum NT-proBNP levels are associated with microstructural MR imaging markers of subclinical brain damage (difference in standardized fractional anisotropy per standard deviation increase in NT-proBNP, −0.048; $P = .019$; difference in standardized mean diffusivity per standard deviation increase in NT-proBNP, 0.054; $P = .004$).

Materials and Methods

Study Population

This study was conducted within the Rotterdam Study, an ongoing prospective population-based cohort of persons living in the geographically defined Ommoord district in Rotterdam, the Netherlands. The cohort originated in 1990 and comprised 7983 participants aged at least 55 years. In 2000 and 2006, the cohort was expanded and now comprises 14926 participants aged at least 45 years (14). Brain MR imaging was implemented from 2005 on (15), and a random subset had serum samples collected around the time of MR imaging (median interval, 21 days; interquartile range, 13–39 days). NT-proBNP was measured between 2006 and 2009 in 2824 participants who underwent brain MR imaging. We excluded participants with prevalent clinical stroke ($n = 34$); those with prevalent dementia based on a three-step protocol described in detail previously (16); those in whom screening was insufficient to determine if the subject had dementia ($n = 35$); those with prevalent overt heart disease, including a clinical diagnosis of heart failure, atrial fibrillation, or coronary heart disease (17) ($n = 146$); those with insufficient follow-up data for overt heart disease ($n = 56$); and those with an NT-proBNP level higher than the age-specific heart failure limit (54 pmol/L in patients younger than 50 years; 108 pmol/L in patients aged 50–75 years; 216 pmol/L in patients older than 75 years) (18) ($n = 3$) to be able to explore the association between NT-proBNP and brain disease in a subclinical population. Furthermore, we excluded participants with inadequate MR image quality ($n = 88$) or cortical brain infarcts on MR images ($n = 55$). In total, 2397 participants were included for analysis (Fig E1 [online]). The Rotterdam Study has been approved by the medical ethics

Published online before print
10.1148/radiol.2016160548 **Content code:** NR

Radiology 2017; 283:205–214

Abbreviations:
CI = confidence interval
eGFR = estimated glomerular filtration rate
NT-proBNP = N-terminal pro–B-type natriuretic peptide
WML = white matter lesion

Author contributions:
Guarantors of integrity of entire study, M.A.I., M.W.V.; study concepts/study design or data acquisition or data analysis/interpretation, all authors; manuscript drafting or manuscript revision for important intellectual content, all authors; approval of final version of submitted manuscript, all authors; agrees to ensure any questions related to the work are appropriately resolved, all authors; literature research, M.W.V.; clinical studies, M.A.I., A.v.d.L., M.W.V.; statistical analysis, H.I.Z., M.A.I.; and manuscript editing, all authors

Conflicts of interest are listed at the end of this article.

committee in accordance with the Population Study Act Rotterdam Study executed by the Ministry of Health, Welfare and Sports of the Netherlands. Written informed consent was obtained from all participants.

NT-proBNP Measurement

Blood samples for NT-proBNP assessment were collected in glass tubes containing clot activator and gel for serum separation and were stored at −80°C. NT-proBNP level was determined by using a commercially available electrochemiluminescence immunoassay (Elecsys proBNP; F Hoffman-La Roche, Basel, Switzerland) and an Elecsys 2010 analyzer (19). Precision, analytic sensitivity, and stability of the system have been described elsewhere (20).

MR Imaging

Brain MR imaging was performed with a 1.5-T MR imager (Signa Excite II; GE Healthcare, Milwaukee, Wis) and an eight-channel head coil. In short, the following sequences were performed: T1-weighted imaging, proton density–weighted imaging, fluid-attenuated inversion recovery imaging, three-dimensional T2* gradient-echo imaging, and diffusion-tensor imaging (15). More details are provided in Appendix E1 (online).

Markers of Subclinical Brain Damage

Automated tissue segmentation, including the conventional k-nearest neighbor brain tissue classifier extended with white matter lesion (WML) segmentation, was used to segment the brain into gray matter, white matter, WML, and cerebrospinal fluid (21). Total brain volume was defined as the sum of gray matter and white matter. White matter was a summation of normal-appearing white matter and WML. Intracranial volume (excluding the cerebellum with surrounding cerebrospinal fluid) was estimated by summing the total gray and white matter volume and cerebrospinal fluid volume. The automated tissue segmentation method has been evaluated extensively, and the accuracy is close to the interobserver variability of manual segmentations (21). According to our study protocol, all images were rated by a group of trained reviewers to determine the presence and location of cortical infarcts, lacunar infarcts, and microbleeds. This group of trained reviewers consisted of researchers with doctor of medicine–level training or training in academic neuropsychology (15,22) (Appendix E1 [online]). Lacunae were rated visually as focal lesions at least 3 mm and less than 15 mm in size, with the same signal intensity as that of cerebrospinal fluid for all sequences and a hyperintense rim on fluid-attenuated inversion recovery images (when located supratentorially) (23). Infarcts showing involvement of gray matter were classified as cortical infarcts. Microbleeds were rated as small focal areas of signal intensity loss on three-dimensional T2* gradient-echo images (23). Intra- and interrater observer reliability testing has been performed for all focal measures, as described previously (15,22).

All diffusion data were preprocessed with a standardized pipeline, including correction for motion and eddy currents. Subsequently, the diffusion tensor was estimated, and the diffusion-tensor imaging data were registered to the tissue segmentation to obtain global mean diffusion-tensor imaging measures in normal-appearing white matter. These measures included fractional anisotropy, mean diffusivity, axial diffusivity, and radial diffusivity (24). In general, lower fractional anisotropy and higher mean diffusivity are indicative of poorer microstructural organization of the white matter.

Volumetric measures comprised total brain, gray matter, white matter, and WML volume. Focal measures comprised lacunar infarcts and microbleeds. Microstructural measures comprised fractional anisotropy and mean diffusivity in normal-appearing white matter. Figure 1 shows an overview of all measures of subclinical brain damage.

Covariates

Information on cardiovascular determinants was obtained during a structured interview by a research nurse at the participants' home, during a physical examination by a research nurse at the research center, and via blood sampling. Body mass index was calculated by dividing weight (in kilograms) by height squared (in meters). Systolic and diastolic blood pressure (in millimeters of mercury) was measured twice with a random-zero sphygmomanometer, and the average of the two measurements was used. Serum glucose, total cholesterol, and high-density lipoprotein cholesterol levels (all in millimoles per liter) were measured with standard laboratory techniques. Diabetes mellitus was defined as a fasting serum glucose level of at least 7.0 mmol/L, a nonfasting serum glucose level of at least 11.1 mmol/L, or use of antidiabetic medication. Smoking habits were assessed in an interview, and participants were categorized as current smokers, former smokers, and those who had never smoked. Information on use of antihypertensive medication and lipid-lowering medication was obtained in an interview. Apolipoprotein E (*APOE*) genotyping was performed for coded genomic DNA samples. *APOE* ε4 carrier status was defined as a person who carried one or two ε4 alleles. Estimated glomerular filtration rate (eGFR) was calculated on the basis of creatinine level by using the chronic kidney disease epidemiology collaboration formula. Cerebral blood flow was measured in 2294 of 2297 (99.9%) participants and was calculated from the phase-contrast images with custom software (Cinetool version 4; GE Healthcare, Milwaukee, Wis), as described previously (25). Total cerebral blood flow was determined by adding flow rates for the carotid arteries and the basilar artery and was expressed in milliliters per minute (25). This method, which is similar to flow measurement methods described previously, has been validated extensively (26).

Statistical Analyses

NT-proBNP level (in picomoles per liter) was first natural log transformed and then was modeled continuously per standard deviation increase. WML volume was natural log transformed and

Figure 1

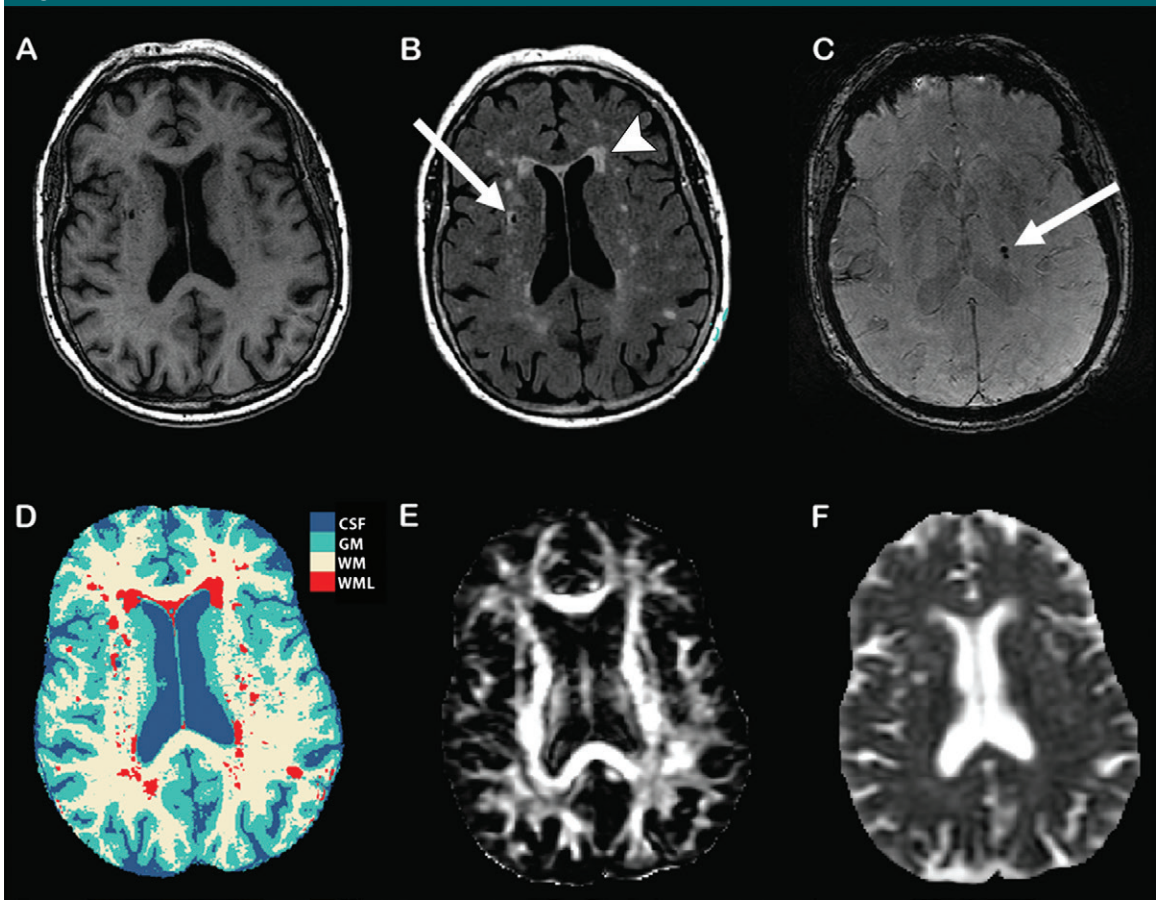

Figure 1: Structural and microstructural MR imaging markers of subclinical brain damage. The left side of each image corresponds to right side of the brain. *A*, T1-weighted image. *B*, Fluid-attenuated inversion recovery image shows WMLs (arrowhead) and lacunar infarct (arrow). *C*, Three-dimensional T2* gradient-echo MR image shows cerebral microbleeds (arrow). *D*, Tissue segmentation, with each tissue type represented by a different color. *CSF* = cerebral spinal fluid, *GM* = gray matter, *WM* = white matter. *E*, Diffusion-tensor imaging map of fractional anisotropy. *F*, Diffusion-tensor imaging map of mean diffusivity.

was investigated continuously. Lacunae and microbleeds were investigated dichotomously (present vs absent). Volumetric measures and diffusion-tensor imaging measures were *z*-standardized (subtracting the mean and dividing by the standard deviation). We used multivariable linear regression models to obtain mean differences in total brain volume, gray matter volume, white matter volume, WML volumes, and diffusion-tensor imaging measures for every standard deviation increase in NT-proBNP. Logistic regression models were used to calculate odds ratios to investigate the association of NT-proBNP with presence of lacunae and microbleeds. In addition, we performed analyses by categories of lacune and microbleed count, assigning participants as having no (reference category) lacunae or microbleeds, one lacuna or microbleed, or two or more lacunae or microbleeds. We performed all analyses in two models. In the first model, we adjusted for age, age^2, and sex. In the second model, we further adjusted for body mass index, systolic and diastolic blood pressure, total and high-density lipoprotein cholesterol level, diabetes mellitus, smoking, antihypertensive and lipid-lowering medication, and *APOE* ε4 carrier status to minimize confounding by cardiovascular disease based on biologic plausibility. Analyses involving volumetric measures were also adjusted for intracranial volume. Gray matter volume and white matter volume were adjusted for each other in analyses. Microstructural measures were adjusted for intracranial volume, normal-appearing white matter, and WML volume.

Also, to compare the magnitude of the association of age as a well-known risk factor for subclinical brain damage, we calculated the effect estimates for the association of age with MR imaging markers of subclinical brain damage. Then, we divided the β values of NT-proBNP (per standard deviation) by the β value of age in relation to markers of subclinical brain disease and reported the corresponding ratios.

Table 1

Characteristics of the Study Population

Characteristic	Total Population(n = 2397)	Tertiles of NT-proBNP (pmol/L)		
		Tertile 1(n = 797)	Tertile 2(n = 802)	Tertile 3(n = 798)
Age (y)	56.6 ± 6.1	54.9 ± 5.0	56.6 ± 5.8	58.2 ± 7.0
Female sex	1379 (57.5)	278 (34.9)	487 (60.7)	614 (76.9)
NT-proBNP level (pmol/L)	5.37 (3.09–9.43)*	0.59–3.77†	3.79–7.81†	7.83–155.50†
Body mass index (kg/m^2)	27.4 ± 4.3	27.8 ± 4.0	27.3 ± 4.2	27.1 ± 4.6
Systolic blood pressure (mmHg)	131.9 ± 18.3	131.1 ± 16.0	130.5 ± 17.7	134.1 ± 20.7
Diastolic blood pressure (mmHg)	82.5 ± 10.7	82.8 ± 9.9	81.7 ± 10.4	83.0 ± 11.8
Total cholesterol level (mmol/L)	5.6 ± 1.0	5.6 ± 1.0	5.6 ± 1.0	5.6 ± 1.1
High-density lipoprotein level (mmol/L)	1.5 ± 0.4	1.3 ± 0.5	1.5 ± 0.4	1.5 ± 0.5
Diabetes mellitus	190 (7.9)	74 (9.3)	62 (7.7)	54 (6.8)
Smoking				
Former smoker	1041 (43.5)	349 (43.8)	358 (44.8)	334 (41.9)
Current smoker	612 (25.6)	218 (27.4)	187 (23.4)	207 (26.0)
Antihypertensive medication	470 (19.8)	121 (15.3)	144 (18.0)	205 (26.0)
Lipid-lowering medication	422 (17.8)	118 (15.0)	136 (17.0)	168 (21.3)
APOE ε4 carrier	670 (30.0)	220 (29.6)	226 (30.1)	224 (30.1)
Creatinine-based eGFR (mL/min/1.73 m^2)	88.6 ± 13.6	90.3 ± 12.0	89.1 ± 13.1	86.3 ± 15.3
Total cerebral blood flow (mL/min)	560 ± 100	572 ± 96	558 ± 102	550 ± 100

Note.—Data are mean ± standard deviation for continuous variables and number of patients for categorical variables. Unless otherwise indicated, data in parentheses are percentages. The following variables had missing data: body mass index (n = 1), blood pressure (n = 10), total cholesterol level (n = 4), high-density lipoprotein cholesterol level (n = 4), smoking history (n = 3), antihypertensive and lipid-lowering medication (n = 23), *APOE* ε4 carrier (n = 160), creatinine-based eGFR (n = 68), and total cerebral blood flow (n = 3).

* Data are median, with interquartile range in parentheses.

† Data are the range.

In sensitivity analyses, we additionally adjusted for eGFR because participants with renal insufficiency may have had higher NT-proBNP levels. Also, we adjusted for total cerebral blood flow as a marker of cerebral perfusion. Furthermore, we computed tertiles of NT-proBNP and compared the highest tertile to the lowest tertile, and we studied linear trends of NT-proBNP in relation to markers of subclinical brain damage. To investigate whether the association between NT-proBNP level and subclinical brain damage was modified by sex, we tested the interaction by adding an interaction term to the regression models. When evaluating linearity assumption, there was no departure from linearity for the linear regression models (normal distribution of residuals) or the logistic regression models (goodness-of-fit statistics). We corrected the P value (α = .05) for multiple comparisons by using the Sidák correction after we estimated the number of independent tests, resulting in a threshold for significance of $P < 5.1 \times 10^{-3}$. All analyses were performed with statistical software (SPSS, version 21.0.0.1; SPSS).

Results

Characteristics of the study population are presented in Table 1. Of the 2397 participants, 57.5% were women (mean age, 56.6 years; age range, 45.7–87.3 years). Median NT-proBNP level was 5.37 pmol/L (interquartile range, 3.09–9.43 pmol/L). Mean total brain volume, gray matter volume, and white matter volume were 963 mL ± 98, 540 mL ± 53, and 423 mL ± 57, respectively. Median WML volume was 2.0 mL (interquartile range, 1.3–3.4 mL). In total, 3.0% of the participants had at least one lacuna, and 11.5% had at least one microbleed. Mean fractional anisotropy was 0.34 (range, 0.25–0.39), and mean diffusivity was 0.73 $\times 10^{-3}$ mm^2/sec (range, [0.67–0.87] $\times 10^{-3}$ mm^2/sec) (Table 2).

Table 3 shows the association between NT-proBNP level and MR imaging markers of subclinical brain disease. In model 1, higher NT-proBNP level was associated with smaller total brain volume (mean difference in z score per standard deviation increase in NT-proBNP level, −0.021; 95% confidence interval [CI]: −0.034, −0.007; P = .003) and is driven predominantly by smaller gray matter volume (mean difference in z score per standard deviation increase in NT-proBNP level, −0.037; 95% CI: −0.057, −0.017; $P < .001$) and less by white matter volume. In model 1, higher NT-proBNP level was associated with larger WML volume (mean difference in z score per standard deviation increase in NT-proBNP level: 0.090; 95% CI: 0.051, 0.129; $P < .001$), with lower fractional anisotropy and higher mean diffusivity in the white matter (Table 3, Table E1 [online]). No associations were found between NT-proBNP level and lacunae or cerebral microbleeds. Estimates

Table 2

MR Imaging Markers of Subclinical Brain Damage

MR Imaging Marker	Total Population (n = 2397)
Total brain volume (mL)	963 ± 98
Gray matter volume (mL)	540 ± 53
White matter volume (mL)	423 ± 57
WML volume (mL)	2.0 (1.3–3.4)*
No. of lacunae	73 (3.0)
One	55 (2.3)
Two or more	18 (0.8)
No. of microbleeds	274 (11.4)
One	215 (9.0)
Two or more	59 (2.5)
Fractional anisotropy	0.34 (0.01)
Diffusivity ($\times 10^{-3}$ mm^2/sec)	
Mean	0.73 ± 0.02
Radial	0.59 ± 0.02
Axial	1.00 ± 0.02

Note.—Data are mean ± standard deviation for continuous variables and number of patients, with percentage in parentheses, for categorical variables. The following variables had missing data: fractional anisotropy and mean diffusivity (n = 53) and radial diffusivity and axial diffusivity (n = 35). Cerebral microbleeds were measured in 2383 participants (14 scans were excluded because susceptibility-weighted images were of inadequate quality).

*Data are median, with interquartile range in parentheses.

Table 3

NT-ProBNP and MR Imaging Markers of Subclinical Brain Damage

Characteristic	Model 1	Model 2
Volumetric measures		
Total brain volume	−0.021 (−0.034, −0.007)*	−0.017 (−0.031, −0.002)
Gray matter volume	−0.037 (−0.057, −0.017)*	−0.031 (−0.052, −0.009)*
White matter volume	−0.020 (−0.041, 0.002)	−0.015 (−0.037, 0.008)
WML volume	0.090 (0.051, 0.129)*	0.076 (0.035, 0.117)*
Focal measures		
Lacunae	1.155 (0.893, 1.492)	1.033 (0.784, 1.362)
0 vs 1	1.167 (0.869, 1.568)	1.066 (0.772, 1.471)
0 vs ≥2	1.103 (0.669, 1.821)	0.890 (0.530, 1.495)
Cerebral microbleeds	1.036 (0.900, 1.192)	1.011 (0.867, 1.179)
0 vs 1	1.035 (0.885, 1.210)	1.019 (0.861, 1.207)
0 vs ≥2	1.038 (0.780, 1.380)	0.976 (0.703, 1.354)
Microstructural measures		
Fractional anisotropy	−0.048 (−0.088, −0.008)	−0.043 (−0.085, −0.000)
Mean diffusivity ($\times 10^{-3}$ mm^2/sec)	0.054 (0.018, 0.091)*	0.051 (0.012, 0.090)

Note.—For volumetric measures, data are mean differences (z scores). For lacunae and microbleeds, data are odds ratios for lacunae or microbleeds per 1-standard-deviation increase in NT-proBNP. For microstructural measures, data are mean differences (z scores) for fractional anisotropy and mean diffusivity per 1-standard-deviation increase in NT-proBNP level. All data in parentheses are 95% CIs. Model 1 was adjusted for age, age^2, and sex. Model 2 also was adjusted for age, age^2, and sex, and was additionally adjusted for body mass index, systolic and diastolic blood pressure, total and high-density lipoprotein cholesterol level, diabetes mellitus, smoking history, use of antihypertensive or lipid-lowering medication, and status as an *APOE* ε4 carrier. Analyses involving volumetric measures were additionally adjusted for intracranial volume. Gray and white matter volumes were adjusted for each other. Microstructural measures were additionally adjusted for intracranial volume and macrostructural white matter measures (normal-appearing white matter and WML volume). Analyses in model 2 were performed as a complete case analysis.

* Data are significantl after correction for multiple testing.

were slightly attenuated by additional adjustment for cardiovascular risk factors and *APOE* ε4 carrier status (model 2), such that associations with total brain volume and mean diffusivity remained significant but did not survive correction for multiple testing (Table 3).

When we compared the effect estimates of NT-proBNP level in relation to markers of subclinical brain damage with the estimates for age, we found that each 1-standard-deviation increase in NT-proBNP level corresponded to a 1.2-year increase in age for gray matter volume, a 1.4-year increase in age for WML volume, and a 3.9-year increase in age for fractional anisotropy (Table E2 [online]).

Furthermore, adjustment for eGFR and total cerebral blood flow did not alter any of the aforementioned results (Tables E3, E4 [online]).

Figure 2 shows the association of NT-proBNP level in tertiles with volumetric, focal, and microstructural measures (model 2). Participants in the highest tertile of NT-proBNP level had lower gray matter volume, higher WML volume, and higher mean diffusivity of normal-appearing white matter compared with those in the lowest tertile ($P < .05$ for all linear trend tests).

There was no difference between men and women for the association between NT-proBNP level and subclinical brain damage ($P > .05$ for all interactions) (data not shown).

Discussion

In this population-based study of participants without dementia who were free of overt cardiovascular disease, we found that higher serum NT-proBNP level was associated with smaller total brain volume, was predominantly driven by smaller gray matter volume, had a larger WML volume, and had poorer microstructural organization of the normal-appearing white matter, independent of potential confounding variables. Our findings imply that the heart and brain are intimately linked, even in presumably healthy individuals.

Although several studies have shown cardiac dysfunction is associated with stroke and dementia, only a few studies have addressed the link between NT-proBNP level and markers of subclinical brain damage. We found that higher NT-proBNP level was associated with smaller total brain volume and gray matter volume, a finding that was in line with findings of the Age Gene/Environment Susceptibility-Reykjavik Study on community-dwelling elderly persons (27). A study of Framingham offspring who had not experienced a stroke found no association between B-type natriuretic peptide level and parenchymal volumes (28). In a study of patients with diabetes, NT-proBNP level

Figure 2

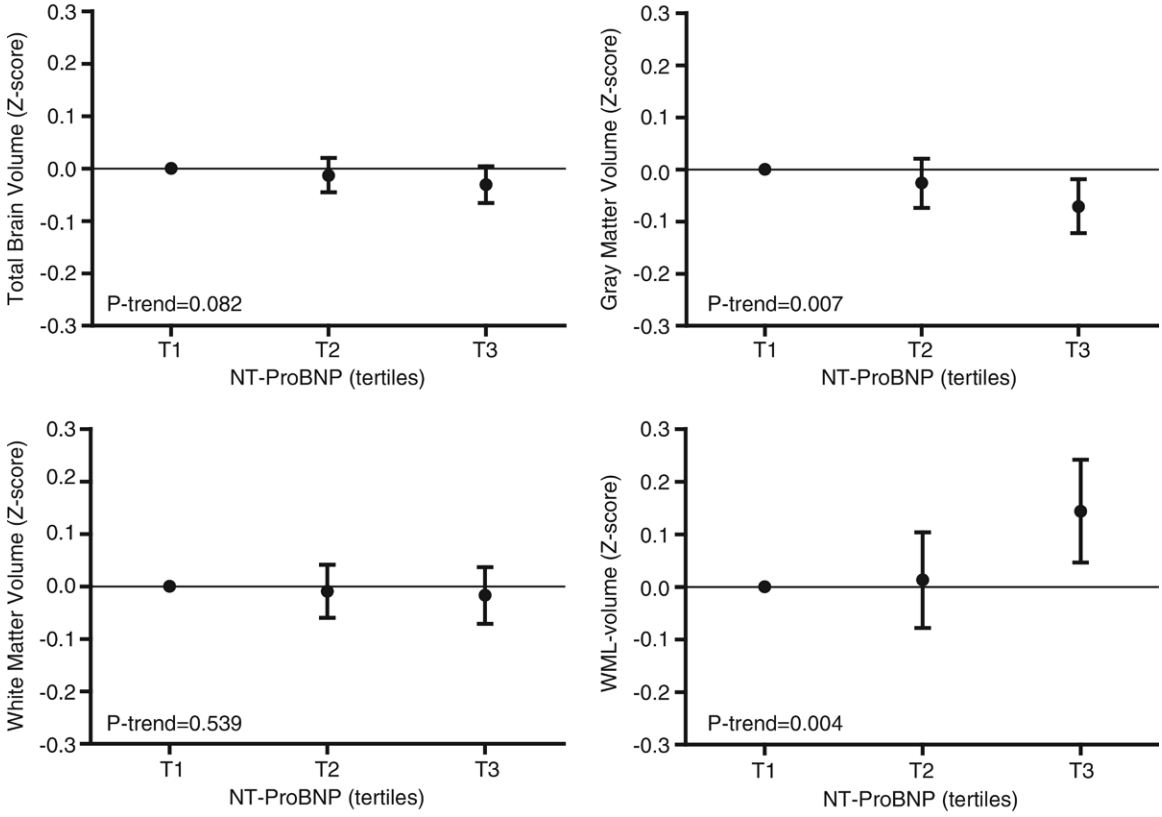

a.

Figure 2: Tertiles of NT-proBNP and MR imaging markers of subclinical brain damage. **(a)** NT-proBNP and volumetric measures. The x-axis shows tertiles of standardized NT-proBNP. The lowest tertile was used as the reference category. ● = mean differences in volumetric measures; bars represent the 95% CI. Analyses involving volumetric measures were additionally adjusted for intracranial volume. Gray matter volume and white matter volume were adjusted for each other. Results in bold were significant after correction for multiple testing ($P < 5.1 \times 10^{-3}$). The range of NT-proBNP for each tertile was 0.59–3.77 pmol/L for tertile 1, 3.79–7.81 pmol/L for tertile 2, and 7.83–155.50 pmol/L for tertile 3 *(Fig 2 continues).*

was associated with higher WML volume (29). The Atherosclerosis Risk in Communities Study found that participants in the highest NT-proBNP quartile had more silent brain infarcts and larger WML volume (30). We did not find an association between higher NT-proBNP level and presence of lacunae or cerebral microbleeds. This discrepancy may be due to a lack of statistical power in our study. Second, presence of lacunae and cerebral microbleeds may mark more downstream neuropathology or, alternatively, it may mark different neuropathology. Third, differences in ethnicity of study populations may yield different cardiovascular risk profiles.

The association between NT-proBNP level and microstructural MR imaging markers has not been well established in the literature. Interestingly, NT-proBNP corresponded to larger increases in age for the microstructural markers than for the macrostructural markers. There is evidence that microstructural brain changes precede macrostructural brain changes (eg, white matter atrophy, WML); thus, they may indicate more subtle brain disease (31). White matter microstructure has been shown to be of great importance for cognitive function, gait, and basic activities of daily living (4). We found that a higher serum NT-proBNP level was associated with poorer microstructural organization of normal-appearing white matter and that this association was independent of the presence of atrophy and WML. This suggests that changes in the normal-appearing white matter organization, which are invisible at conventional MR imaging, are associated with subclinical cardiac dysfunction. The fact that the association between NT-proBNP level and white matter macrostructure was most pronounced in WML rather than white matter volume might suggest different pathophysiologic processes that underlie white matter atrophy and WML.

Several mechanisms have been proposed to explain the link between

Figure 2 (continued)

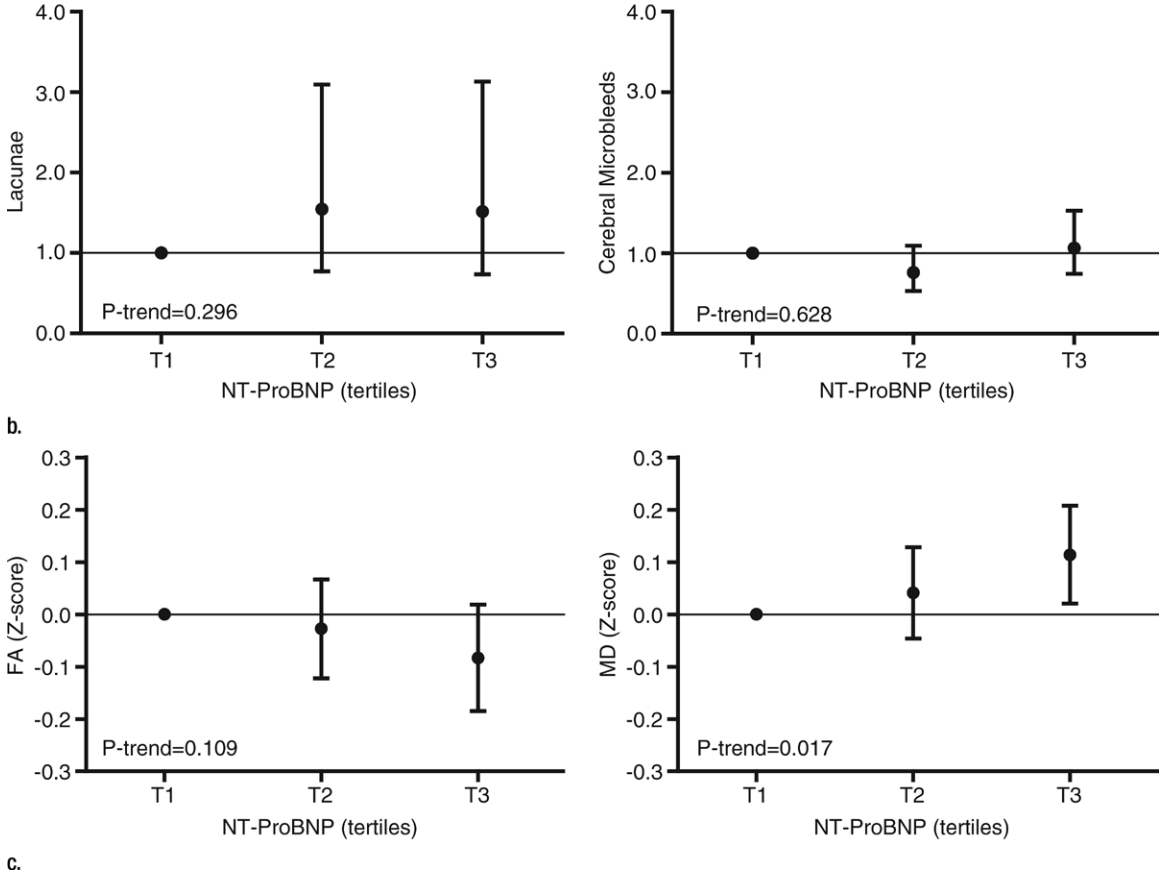

Figure 2 *(continued).* **(b)** NT-proBNP and focal measures. **(c)** NT-proBNP and microstructural measures. The x-axis shows tertiles of standardized NT-proBNP. The lowest tertile was used as the reference category. ● = odds ratios for focal measures (**b**), and mean differences in microstructural measures (**c**); bars represent the 95% CI. Microstructural measures were additionally adjusted for intracranial volume and macrostructural white matter measures (normal-appearing white matter and WML volume). Results in bold were significant after correction for multiple testing ($P < 5.1 \times 10^{-3}$). The range of NT-proBNP for each tertile was 0.59–3.77 pmol/L for tertile 1, 3.79–7.81 pmol/L for tertile 2, and 7.83–155.50 pmol/L for tertile 3.

cardiac dysfunction and clinical or subclinical brain disease. A direct mechanism by which NT-proBNP itself causes brain disease is highly unlikely since NT-proBNP is not known to be neurotoxic. Potential indirect mechanisms include cerebral hypoperfusion, shared cardiovascular risk factors, cardioembolic stroke, and ischemia due to atherosclerosis.

First, maintaining continuous cerebral perfusion is essential for normal brain function. Experimental evidence from animal studies suggests that cerebral hypoperfusion leads to cerebral microvascular damage, neuropathologic processes, and cognitive decline, supporting the concept that cerebral hypoperfusion precedes neurodegeneration (32). When investigating NT-proBNP with gray and white matter volumes, we observed the strongest association with gray matter volume. Because gray matter is more metabolically active than white matter, it requires more cerebral blood flow (32). Thus, cerebral hypoperfusion may have a greater effect on gray matter volume than on white matter volume. Interestingly, adjustment for total cerebral blood flow as an indicator for cerebral perfusion did not alter the associations in our analyses. A possible explanation for this might be that although our cerebral blood flow measurement was extensively validated previously, it is still rather coarse and may not cancel out all variability in brain perfusion. In addition, cerebral blood flow measurement is obtained at only one time point; thus, it might not be fully representative of cerebral perfusion.

As a second explanatory mechanism, the brain relies on several hemodynamic parameters, such as cerebral autoregulation, including endothelial function and cardiac output, to meet its metabolic demands (33). There is evidence that cardiovascular risk factors may cause concurrent endothelial dysfunction in the heart and brain that

may lead to problems in maintaining microcirculation and blood-brain barrier function (34). Remarkably, in our study, adjustments for cardiovascular risk factors did not essentially alter the associations. However, we cannot rule out the possibility of residual confounding due to an unmeasured (cardiovascular) risk factor.

Third, cardioembolic stroke from paroxysmal atrial fibrillation that is not picked up at diagnostic electrocardiography also may affect the brain due to hemodynamic compromise (35). The largest effect was detected for WML volume. It has been hypothesized that atherosclerosis causes arterial stiffness, which may limit the perfusion of the brain and heart. Indeed, on the one hand, arterial stiffness has been associated with markers of brain disease, such as larger WML volume, presence of lacunae, and cortical brain atrophy (36,37). On the other hand, arterial stiffness has been associated with cardiovascular morbidity and mortality (38). Lastly, it has been hypothesized that B-type natriuretic peptide is secreted in response to systemic inflammatory factors (39). Inflammatory factors may damage the blood brain barrier, which may cause increased permeability resulting in WMLs, cerebral microbleeds, and lacunar infarcts (40).

There are also some limitations that must be acknowledged. First, ours was a cross-sectional study; thus, we could not draw conclusions regarding causality or the direction of the associations. However, from a biologic perspective, and on the basis of animal studies, it is more likely that cardiac dysfunction affects brain changes than vice versa (6). Second, our study consisted largely of white participants, and this may have limited extrapolation of our results to patients of other ethnicities.

In conclusion, we found that in community-dwelling middle-aged and elderly persons, subclinical cardiac dysfunction as reflected by serum NT-proBNP levels is associated with global and microstructural MR imaging markers of subclinical brain damage. Our findings suggest that the heart and brain are intimately linked, even in presumably healthy individuals. This is essential since cardiac dysfunction and subclinical brain damage are growing problems. Further research is needed to elucidate the causal relationship between cardiac dysfunction and subclinical brain disease and to explore the prevailing pathway among several hypotheses. Additionally, it may be interesting to investigate whether NT-proBNP can be used as a clinically relevant marker for subclinical brain damage.

Disclosures of Conflicts of Interest: H.I.Z. disclosed no relevant relationships. **M.A.I.** disclosed no relevant relationships. **A.H.** disclosed no relevant relationships. **W.J.N.** Activities related to the present article: is the cofounder and chief scientific officer of and a shareholder in Quantib. Activities not related to the present article: has a patent application pending for visualizing imaging biomarker extraction results. Other relationships: disclosed no relevant relationships. **A.v.d.L.** disclosed no relevant relationships. **G.P.K.** Activities related to the present article: disclosed no relevant relationships. Activities not related to the present article: is a consultant for Bracco and received grants from Siemens, Bayer, GE Healthcare, and Bracco. Other relationships: disclosed no relevant relationships. **O.H.F.** Activities related to the present article: disclosed no relevant relationships. Activities not related to the present article: received grants from Metagenics and Nestle. Other relationships: disclosed no relevant relationships. **M.W.V.** disclosed no relevant relationships.

References

1. Mozaffarian D, Benjamin EJ, Go AS, et al. Heart disease and stroke statistics--2015 update: a report from the American Heart Association. Circulation 2015;131(4):e29–e322.
2. Wortmann M. Dementia: a global health priority - highlights from an ADI and World Health Organization report. Alzheimers Res Ther 2012;4(5):40.
3. Rostamian S, Mahinrad S, Stijnen T, Sabayan B, de Craen AJ. Cognitive impairment and risk of stroke: a systematic review and meta-analysis of prospective cohort studies. Stroke 2014;45(5):1342–1348.
4. Verlinden VJ, van der Geest JN, de Groot M, et al. Structural and microstructural brain changes predict impairment in daily functioning. Am J Med 2014;127(11):1089–96.e2 .
5. van Buchem MA, Biessels GJ, Brunner la Rocca HP, et al. The heart-brain connection: a multidisciplinary approach targeting a missing link in the pathophysiology of vascular cognitive impairment. J Alzheimers Dis 2014;42(Suppl 4):S443–S451.
6. Qiu C, Fratiglioni L. A major role for cardiovascular burden in age-related cognitive decline. Nat Rev Cardiol 2015;12(5):267–277.
7. Dutta M, Hanna E, Das P, Steinhubl SR. Incidence and prevention of ischemic stroke following myocardial infarction: review of current literature. Cerebrovasc Dis 2006;22(5-6):331–339.
8. Medi C, Hankey GJ, Freedman SB. Stroke risk and antithrombotic strategies in atrial fibrillation. Stroke 2010;41(11):2705–2713.
9. Haeusler KG, Laufs U, Endres M. Chronic heart failure and ischemic stroke. Stroke 2011;42(10):2977–2982.
10. Daniels LB, Maisel AS. Natriuretic peptides. J Am Coll Cardiol 2007;50(25):2357–2368.
11. McDonagh TA, Robb SD, Murdoch DR, et al. Biochemical detection of left-ventricular systolic dysfunction. Lancet 1998;351(9095):9–13.
12. Mirza SS, de Bruijn RF, Koudstaal PJ, et al. The N-terminal pro B-type natriuretic peptide, and risk of dementia and cognitive decline: a 10-year follow-up study in the general population. J Neurol Neurosurg Psychiatry 2016;87(4):356–362.
13. Portegies ML, Kavousi M, Leening MJ, et al. N-terminal pro-B-type natriuretic peptide and the risk of stroke and transient ischaemic attack: the Rotterdam Study. Eur J Neurol 2015;22(4):695–701.
14. Hofman A, Brusselle GG, Darwish Murad S, et al. The Rotterdam Study: 2016 objectives and design update. Eur J Epidemiol 2015;30(8):661–708.
15. Ikram MA, van der Lugt A, Niessen WJ, et al. The Rotterdam Scan Study: design update 2016 and main findings. Eur J Epidemiol 2015;30(12):1299–1315.
16. Schrijvers EM, Verhaaren BF, Koudstaal PJ, Hofman A, Ikram MA, Breteler MM. Is dementia incidence declining?: Trends in dementia incidence since 1990 in the Rotterdam Study. Neurology 2012;78(19):1456–1463.
17. Leening MJ, Kavousi M, Heeringa J, et al. Methods of data collection and definitions of cardiac outcomes in the Rotterdam Study. Eur J Epidemiol 2012;27(3):173–185.
18. Januzzi JL, van Kimmenade R, Lainchbury J, et al. NT-proBNP testing for diagnosis and short-term prognosis in acute destabilized heart failure: an international pooled analysis of 1256 patients: the International Collaborative of NT-proBNP Study. Eur Heart J 2006;27(3):330–337.

19. Rutten JH, Mattace-Raso FU, Steyerberg EW, et al. Amino-terminal pro-B-type natriuretic peptide improves cardiovascular and cerebrovascular risk prediction in the population: the Rotterdam study. Hypertension 2010;55(3):785–791.

20. Yeo KT, Wu AH, Apple FS, et al. Multicenter evaluation of the Roche NT-proBNP assay and comparison to the Biosite Triage BNP assay. Clin Chim Acta 2003;338(1-2):107–115.

21. de Boer R, Vrooman HA, van der Lijn F, et al. White matter lesion extension to automatic brain tissue segmentation on MRI. Neuroimage 2009;45(4):1151–1161.

22. Vernooij MW, Ikram MA, Tanghe HL, et al. Incidental findings on brain MRI in the general population. N Engl J Med 2007;357(18):1821–1828.

23. Vernooij MW, van der Lugt A, Ikram MA, et al. Prevalence and risk factors of cerebral microbleeds: the Rotterdam Scan Study. Neurology 2008;70(14):1208–1214.

24. Koppelmans V, de Groot M, de Ruiter MB, et al. Global and focal white matter integrity in breast cancer survivors 20 years after adjuvant chemotherapy. Hum Brain Mapp 2014;35(3):889–899.

25. Vernooij MW, van der Lugt A, Ikram MA, et al. Total cerebral blood flow and total brain perfusion in the general population: the Rotterdam Scan Study. J Cereb Blood Flow Metab 2008;28(2):412–419.

26. Spilt A, Box FM, van der Geest RJ, et al. Reproducibility of total cerebral blood flow measurements using phase contrast magnetic resonance imaging. J Magn Reson Imaging 2002;16(1):1–5.

27. Sabayan B, van Buchem MA, de Craen AJ, et al. N-terminal pro-brain natriuretic peptide and abnormal brain aging: The AGES-Reykjavik Study. Neurology 2015;85(9):813–820.

28. Pikula A, Beiser AS, DeCarli C, et al. Multiple biomarkers and risk of clinical and subclinical vascular brain injury: the Framingham Offspring Study. Circulation 2012;125(17):2100–2107.

29. Reinhard H, Garde E, Skimminge A, et al. Plasma NT-proBNP and white matter hyperintensities in type 2 diabetic patients. Cardiovasc Diabetol 2012;11:119.

30. Dadu RT, Fornage M, Virani SS, et al. Cardiovascular biomarkers and subclinical brain disease in the atherosclerosis risk in communities study. Stroke 2013;44(7):1803–1808.

31. de Groot M, Verhaaren BF, de Boer R, et al. Changes in normal-appearing white matter precede development of white matter lesions. Stroke 2013;44(4):1037–1042.

32. Farkas E, Luiten PG, Bari F. Permanent, bilateral common carotid artery occlusion in the rat: a model for chronic cerebral hypoperfusion-related neurodegenerative diseases. Brain Res Brain Res Rev 2007;54(1):162–180.

33. de la Torre JC. Critically attained threshold of cerebral hypoperfusion: the CATCH hypothesis of Alzheimer's pathogenesis. Neurobiol Aging 2000;21(2):331–342.

34. de la Torre JC. Cardiovascular risk factors promote brain hypoperfusion leading to cognitive decline and dementia. Cardiovasc Psychiatry Neurol 2012;2012:367516 .

35. Wachter R, Lahno R, Haase B, et al. Natriuretic peptides for the detection of paroxysmal atrial fibrillation in patients with cerebral ischemia--the Find-AF study. PLoS One 2012;7(4):e34351.

36. Tsao CW, Seshadri S, Beiser AS, et al. Relations of arterial stiffness and endothelial function to brain aging in the community. Neurology 2013;81(11):984–991.

37. King KS, Chen KX, Hulsey KM, et al. White matter hyperintensities: use of aortic arch pulse wave velocity to predict volume independent of other cardiovascular risk factors. Radiology 2013;267(3):709–717.

38. Vlachopoulos C, Aznaouridis K, Stefanadis C. Prediction of cardiovascular events and all-cause mortality with arterial stiffness: a systematic review and meta-analysis. J Am Coll Cardiol 2010;55(13):1318–1327.

39. Shor R, Rozenman Y, Bolshinsky A, et al. BNP in septic patients without systolic myocardial dysfunction. Eur J Intern Med 2006;17(8):536–540.

40. Rouhl RP, Damoiseaux JG, Lodder J, et al. Vascular inflammation in cerebral small vessel disease. Neurobiol Aging 2012;33(8):1800–1806.